Penn Libraries
UNIVERSITY of PENNSYLVANIA

University of Pennsylvania
ScholarlyCommons

Departmental Papers (MSE)

Department of Materials Science & Engineering

December 2002

Imaging, Structural and Chemical Analysis of Silicon Nanowires

R. J. Barsotti Jr.
Massachusetts Institute of Technology

John E. Fischer
University of Pennsylvania, fischer@seas.upenn.edu

C. H. Lee
Korea Advanced Institute of Science and Technology

J. Mahmood
University of Pennsylvania, jmahmood@seas.upenn.edu

Kofi W. Adu
Pennsylvania State University

See next page for additional authors

Follow this and additional works at: http://repository.upenn.edu/mse_papers

Imaging, Structural and Chemical Analysis of Silicon Nanowires

Abstract

Laser ablation has been used to grow silicon nanowires with an average diameter of 6.7 nm ± 2.7 nm surrounded by an amorphous SiO_x sheath of 1-2 nm. This paper reports the imaging, chemical and structural analysis of these wires. Due to the growth temperature and the presence of calcium impurities and trace oxygen, two distinct types of wires are found. They appear to grow by two different processes. One requires a metal catalyst, the other is catalyzed by oxygen.

Author(s)

R. J. Barsotti Jr., John E. Fischer, C. H. Lee, J. Mahmood, Kofi W. Adu, and Peter C. Eklund

Imaging, Structural and Chemical Analysis of Silicon Nanowires

R. J. Barsotti, Jr.[1#], J. E. Fischer[1,*], C. H. Lee[1&], J. Mahmood[1], C. K. W. Adu[2] and P. C. Eklund[2,3]

[1]Department of Materials Science and Engineering, University of Pennsylvania, Philadelphia, PA 19104

[2]Department of Physics, The Pennsylvania State University, University Park, PA 16802

[3]Department of Materials Science and Engineering, The Pennsylvania State University, University Park, PA 16802

[#] Current address: Department of Materials Science and Engineering, Massachusetts Institute of Technology, Cambridge, MA 02139

&Current address: Department of Material Science and Engineering, KAIST, Daejon, Korea

*fischer@sol1.lrsm.upenn.edu

ABSTRACT

Laser ablation has been used to grow silicon nanowires with an average diameter of 6.7 nm $\pm$ 2.7 nm surrounded by an amorphous SiO_x sheath of 1-2 nm. This paper reports the imaging, chemical and structural analysis of these wires. Due to the growth temperature and the presence of calcium impurities and trace oxygen, two distinct types of wires are found. They appear to grow by two different processes. One requires a metal catalyst, the other is catalyzed by oxygen.

INTRODUCTION

Over the past ten years, interest has grown in one-dimensional nanostructures in both academic and industrial communities. Semiconducting nanowires have controllable electronic properties making them a leading candidate for applications [1-6]. Here we report the structural and chemical characterization of small-diameter semiconducting nanowires and propose a growth mechanism based on this analysis.

EXPERIMENTAL DETAILS

Nanowire material was prepared using the pulsed laser vaporization (PLV) technique [7-10]. A mixture of Si (90 at.%) and Fe (10 at.%) powders were hot pressed into a disc 12 mm in diameter and 8 mm thick. This target was placed in the center of a 25 mm diameter quartz tube which could be heated to 1100° C. During growth, preheated argon flowed down the tube at a rate of 100 sccm at 500 Torr. A Nd:YAG laser (model SL803, Spectron Laser Systems) with 1064 nm (850 mJ/pulse) and 532 nm (350 mJ/pulse) at 10 Hz repetition rate was used to ablate the target by rastering the beam with a motorized lens. The 1064 nm pulse was delayed by 50 nanoseconds relative to the 532 nm pulse. The argon gas reversed the flow of the Si/Fe vapor. Nanowire material was found deposited on the walls of the tube for a distance of up to 10 cm behind the target. This PLV method produced silicon nanowires with an average diameter of 6.7 nm

± 2.7 nm surrounded by an amorphous SiO_x sheath of 1-2 nm, comparable in dimension to those produced by a similar method by Lieber[7]. Similarly, Si-Ge nanowires were prepared from a target of Si (45 at. %), Ge (45 at. %) and Au (5 at. %) at a synthesis temperature of 1050˚ C. Ge nanowires were prepared from a target of Ge (95 at. %) and Au (5 at. %) at a temperature of 1050 ˚C. For microscopy studies, the nanowire material was sonicated and dispersed in ethanol.

DISCUSSION

Imaging and analysis was performed on a JEOL 2010 transmission electron microscope. We found and studied two types of silicon nanowires; isolated longer nanowires (5-10 μm) which have few attached nanoparticles, and clustered shorter wires (100-500 nm) connected by many nanoparticles, forming nanochains (Figure 1). Of particular interest are the 360° loops with diameters as small as 100 nm (Figure 1 (B)). Electron beam diffraction on Si nanowire loops demonstrate that the straight segments of the nanowires are crystalline while the areas of high curvature are amorphous. This may indicate that a short segment of the crystalline wire entered a high temperature zone during growth and melted. The wire deformed due to its weight and was quenched in an amorphous state. Similar loops were formed in the TEM when the electron beam was focused on a small spot of a thin Si nanowire.

Chemical analysis was performed with energy dispersive spectroscopy (EDS) in scanning transmission electron microscopy (STEM) mode. The Si nanowires contained silicon and oxygen, suggesting a silicon core surrounded by a SiO_x sheath. The particles which had been assumed to be $FeSi_2$ showed a significant amount of Ca (Figure 1 (D)) but no Fe. Ca-Si particles were found at the end of longer nanowires; nanochains also contained many mid-chain Si-Ca nanoparticles. The balls used to mill and mix the Fe and Si powders were found to be the source of Ca contamination. Nanoparticles which contained only Si and O were found as part of the nanochains.

The morphology and chemical analysis suggest that the Si nanowires were grown
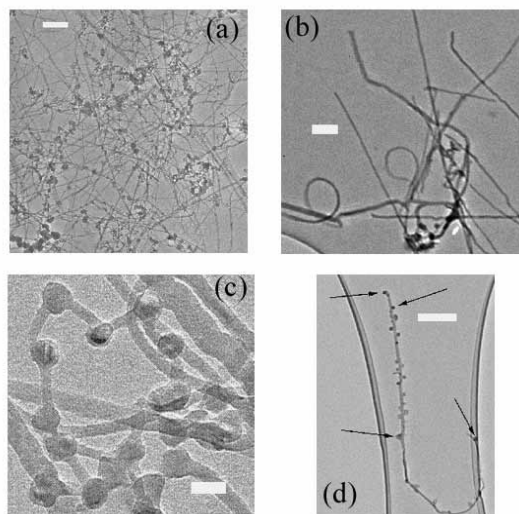

Figure 1: (A) Low magnification TEM image of silicon nanowires; scale bar: 200 nm. (B) TEM image of 5-10 micron long nanowires showing 360° loops; scale bar: 100 nm. (C) STEM image of nanochains; scale bar: 25 nm. (D) Arrows indicate Ca-Si nanoparticles; scale bar: 250 nm.

by two separate mechanisms. The 5-10 micron long nanowires appear to grow via the vapor-liquid-solid mechanism (VLS) (Figure 2 (A)) [7, 11]. Growth is expected to terminate when the catalyst particle crystallizes into $FeSi_2$ or $CaSi_2$. Ca-Si has a lower eutectic temperature of 1030° C (61.4 wt.% Si) compared to 1207° C for Fe-Si (58.2 wt.% Si). This may favor growth by Ca catalysis at the growth temperature of 1100° C.

The VLS model cannot explain the growth of nanochains. The oxide assisted growth mode1 [9, 12-14] (Figure 2 (B)) applied to a laser ablation system where Si, O and Ca are present, can account for the growth of nanochains. SiO_x vapor is formed by the ablation of oxidized Si grains in the target. SiO_x nanoparticles can nucleate on the side of the quartz tube. SiO_x particles then begin to decompose into Si and SiO_2. A wire of crystalline silicon surrounded by an amorphous SiO_2 sheath is then formed. SiO_x and Si vapor continue to fall on the tip of the nanowire. Decomposition leads to nanowire growth which is restricted to one direction by the SiO_2 sheath. SiO_x may land on the tip and crystallize in a growth direction which is not energetically favorable. Another inhibitor of nanowire nucleation may be the existence of Ca in the SiO_x vapor. Si and O build up around the either the nanowire attempting to grow in an unfavorable growth direction, or the Ca impurity. This causes the formation of large spherical particles, as observed in the nanochains. Additional SiO_x vapor impinges upon the particle, and Si begins to crystallize in a favorable direction, allowing a nanowire to nucleate from the particle.

We propose that the 1100° C target temperature permits growth by both VLS and oxide-assisted mechanisms to occur simultaneously, and that the two mechanisms produce the two distinct types of wires found in the sample: 5-10 micron, long nanowires and nanochains. The measured temperature gradient in the furnace is consistent with the possibility that regions within 10 cm of the target are at 1070° C, allowing for nucleation of silicon nanowires by the oxide assisted model [9]. Areas closer to the target would be at temperatures optimal for VLS growth catalyzed by $CaSi_x$, and possibly also by $FeSi_x$, near 1100° C (if the melting point is depressed by the small particle size). The Si-Ge wires showed a similar morphology consisting of both long nanowires and nanochains. Chemical analysis suggested that the wires followed the above growth mechanisms. In
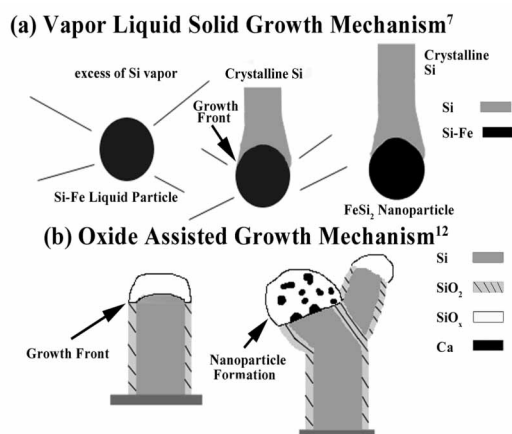

Figure 2: (A) (1) In the VLS growth mechanism, a Si-Fe liquid nanoparticle becomes supersaturated with Si vapor. (2) Crystalline silicon, in thermodynamic equilibrium with the liquid Si-Fe nanoparticle, precipitates out. (3) Growth terminates when the nanoparticle is pushed into a cooler region of the tube, where it crystallizes into $FeSi_2$.
(B) (1) In the Oxide Assisted Growth Model, growth occurs when SiO_x vapor condenses on the side of the quartz tube and decomposes into SiO and SiO_2. Additonal SiO_x vapor lands on the tip of the wire and growth continues in one direction. (2) Nanoparticle formation occurs when calcium vapor inhibits the formation of Si and SiO_2. Renucleation occurs and growth continues along a new direction.
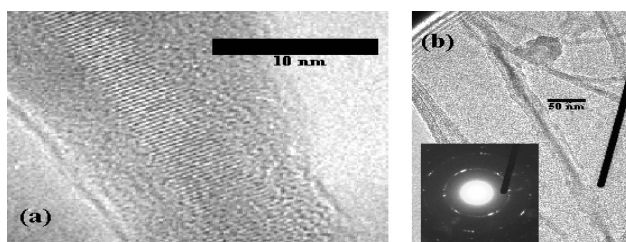
Figure 3: (A) High resolution TEM image showing {111} planes aligned perpendicular to the axis. (B) Electron diffraction of a long, straight nanowire showing <111> growth direction.

the pure Ge samples, only long Ge nanowires, grown via the VLS mechanism, were found. Ge nanowires were grown at a temperature of 1050 C, which is too high for the reported range of favorable temperatures for the oxide assisted growth mechanism of Ge nanowires, 690-705˚ C [13] .

High resolution TEM revealed several other features in the nanowires (Figure 3). The spacing between the lattice fringes in the core of the nanowire is 3.1 Å, signifying that they are Si {111} planes. These are oriented perpendicular to the nanowire axis indicating a <111> growth direction. High resolution TEM images also show nanowires whose {111} planes are oriented at angles of 60°-70° to the growth direction (30°-20° to the perpendicular), suggesting a <211> growth direction as the [211] and [111] directions are 19.47° apart.

Electron diffraction was performed to confirm the growth directions of 5-10 μm Si wires and Si nanochains (Figure 3). Most of the long wires grow in the <111> direction, suggesting that the VLS mechanism favors this growth mode. Si nanochains were found to grow in both <111> and <211> directions, suggesting that oxide-assisted growth does not strongly favor any particular growth direction. High resolution TEM and electron diffraction showed that the Ge nanowires, grown via the VLS mechanism, exhibited a <111> growth direction.

CONCLUSION

In summary, we have reported the imaging and structural analysis of silicon nanowires produced by laser vaporization of Si (90%)- Fe (10%) targets. The nanowires are grown by two distinct growth mechanisms, which were both possible due to growth conditions. The two growth mechanisms produce wires with different morphologies that exhibit different crystallographic growth directions and stem from nanoparticles with different chemical compositions.

REFERENCES

1. Z. Zhang, X. H. Fan, L. Xu, C. S. Lee and S. T. Lee, Chem. Phys. Letters **337**, 18 (2001).
2. J. Yu, S. Chung and J. Heath, J. Phys. Chem. B **104**, 11864 (2000).
3. Y. Cui, X. Duan, J. Hu and C. M. Lieber*,* J. Phys. Chem. B **104**, 5213 (2000).
4. Y. Huang, X. Duan, Q. Wei and C. M. Lieber, Science **291**, 630 (2001).
5. Y. Cui and C. M. Lieber, Science **291**, 851 (2001).
6. Y. Huang, X. Duan, Y. Cui, L. J. Lauhon, K. Kim and C. M. Lieber, Science **294**, 1313 (2001).
7. A.M. Morales and C. M. Lieber, Science **279**, 208 (1998).
8. Y.F. Zhang, Y. H Tang, N. Wang, D. P. Yu, C. S. Lee, I. Bello, and S. T. Lee, Appl. Phys. Letters **72**, 1835 (1998).
9. Y. H. Tang, Y.F. Zhang, N. Wang, W.S. Shi, C.S. Lee, I. Bello and S.T. Lee, J. Vac. Sci. Technol. B **19**, 317 (2001).
10. W. Shi, H. Peng, Y. Zheng, N. Wang, N. Shang, Z. Pan, C. Lee and S. Lee, Adv. Materials **12**, 1343 (2000).
11. R.S. Wagner and W.C. Ellis, Appl. Phys. Letters **4**, 89 (1964).
12. N. Wang, Y.H. Tang, Y.F. Zhang, C.S. Lee, I. Bello and S. T. Lee, Chem. Phys. Letters **299**, 237 (1999).
13. Y.F. Zhang, Y.H. Tang, N. Wang, C.S. Lee, I. Bello and S.T. Lee, J. Crystal Growth **197,** 136 (1999).
14. Y.F. Zhang, Y.H. Tang, C. Lam, N. Wang, C.S. Lee, I. Bello and S.T. Lee, J. Crystal Growth **212**, 115 (2000).